

## Galaxy structure and kinematics towards the NGP

Spagna Alessandro

*INAF-Osservatorio Astronomico di Torino, I-10025 Pino Torinese, Italy*

Cacciari Carla

*INAF - Osservatorio Astronomico di Bologna, I-40127 Bologna*

Drimmel Ronald

*INAF-Osservatorio Astronomico di Torino, I-10025 Pino Torinese, Italy*

Kinman Thomas

*Kitt Peak National Observatory, NOAO, Tucson, AZ 85726-6732, USA*

Lattanzi Mario G.

*INAF-Osservatorio Astronomico di Torino, I-10025 Pino Torinese, Italy*

Smart Richard L.

*INAF-Osservatorio Astronomico di Torino, I-10025 Pino Torinese, Italy*

**Abstract.** We present a proper motion survey over about 200 square degrees towards the NGP, based on the material used for the construction of the GSC-II, that we are using to study the vertical structure and kinematics of the Galaxy. In particular, we measured the rotation velocity of the halo up to 10 kpc above the galactic plane traced by a sample of RR Lyræ and BHB giants for which radial velocities were used to recover the complete distribution of the spatial velocities. Finally, the impact of astrometric and spectroscopic GAIA observation are discussed.

### 1. Introduction

It is generally accepted that the Galaxy is constituted by four discrete main components, the *bulge*, the *thin disk*, the *thick disk* and the *halo*, which are characterized by distinctive stellar populations in terms of spatial distribution, kinematics properties, metallicity and age. A detailed knowledge of such galactic components is essential to achieve a complete description of the Milky Way, as well as of the various processes and evolutionary phases which occurred during the history of our Galaxy (and other galaxies too) and that are responsible for the existence and the properties of those components we observe today.

Ground based surveys providing photometry, proper motions and/or spectroscopic observations have been carried out in the past to study the structure and kinematics of Galactic populations, and these will continue and be extended in the next years thanks to availability of all-sky catalogs such as GSC-II and USNO-B, based on multi-epoch photographic surveys, as well as other current and future photometric and spectroscopic surveys (eg. 2MASS, DENIS, SDSS, EIS, HES, HK, VST, etc.) that benefit from the availability of dedicated scanning and large field cameras as well as large multi-fiber spectrographs (eg. 2dF, 6dF, FLAMES).

Clearly, the GAIA mission will provide an enormous contribution to the understanding of the formation and evolution of the Galaxy, thanks to very accurate astrometric parameters complemented by photometric and spectroscopic measurements which will permit the direct determination of the 6D phase space distribution and the chemical abundance of large and complete samples of stellar tracers belonging to the different galactic components.

Here we describe a new project which combines astrometric, photometric and spectroscopic data in order to investigate the kinematics of the outer halo by means of velocities derived from proper motions and radial velocities for a sample of RR-Lyræ and BHB giants towards the NGP.

## 2. NGP survey: proper motions and radial velocities

At the moment we have surveyed about 200 square degrees towards the NGP, and produced positions, proper motions and photographic photometry for about 500 000 objects down to plate limits ( $R_F < 20.5$ ).

Table 1. Plate material

<i>Survey</i>	<i>Epoch</i>	<i>Pixel</i>	<i>Band</i>	<i>Emulsion + Filter</i>
POSS-I E	1950-1956	25 $\mu\text{m}$	E	103a-E + red plexiglass
POSS-I O	1950-1955	25 $\mu\text{m}$	O	103a-O unfiltered
Quick V	1982-1983	25 $\mu\text{m}$	V <sub>12</sub>	IIaD+Wratten 12
POSS-II J	1988-1996	15 $\mu\text{m}$	B <sub>J</sub>	IIIaJ + GG385
POSS-II F	1989-1996	15 $\mu\text{m}$	R <sub>F</sub>	IIIaF + RG610
POSS-II N	1990-1998	15 $\mu\text{m}$	I <sub>N</sub>	IV-N + RG9

Our material consists of  $6.4^\circ \times 6.4^\circ$  Schmidt plates from the Northern photographic surveys (POSS-I, Quick V and POSS-II) carried out at the Palomar Observatory (Table 1). All plates were digitized at STScI utilizing modified PDS-type scanning machines with 25  $\mu\text{m}$  square pixels (1.7 "/pixel) for the first epoch plates, and 15  $\mu\text{m}$  pixels (1 "/pixel) for the second epoch plates. The digital copies of the plates were initially analyzed by means of the standard software pipeline used for the construction of the GSC-II (see e.g. Lasker et al. 1995 or McLean et al. 2000). The pipeline performs object detection and computes parameters and features for each identified object. Further, the software provides

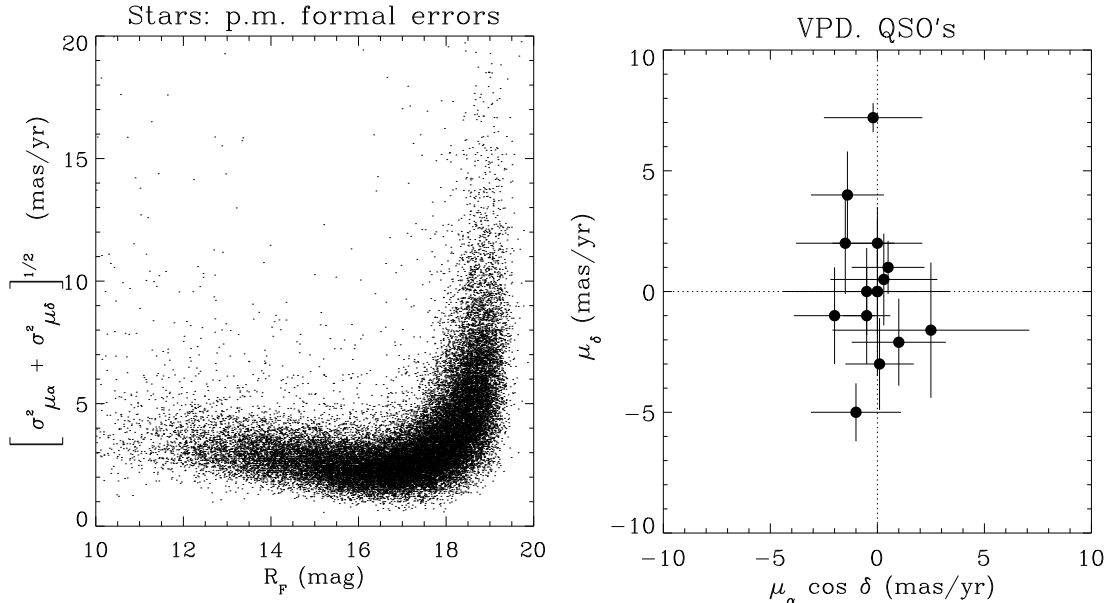


Figure 1. *Left panel.* Formal errors of fitted proper motions as a function of the magnitude (all stellar objects). *Right panel.* Vector point diagram (VPD) of a sample of 15 QSO's, with  $1\sigma$  error bars. Weighted means are  $\langle \mu_\alpha \cos \delta \rangle = -0.02 \pm 0.23$  mas/yr and  $\langle \mu_\delta \rangle = +0.33 \pm 0.28$  mas/yr, respectively. Both plots refer to the POSS-II field no. 442.

classification, position, and magnitude for each object by means of astrometric and photometric calibrations which utilized the Tycho2 (Høg et al. 2000) and the GSPC-2 (Bucciarelli et al. 2001) as reference catalogs. Accuracies better than 0.1-0.2 arcsec in position and 0.15-0.2 mag in photographic magnitude are generally attained. Relative proper motions were derived by applying the procedure described in Spagna et al. (1996) and afterwards transformed to the absolute reference frame forcing the extended extragalactic sources to have null tangential motion. As shown in Figure 1, the typical precision ( $\sigma_\mu \sim 3$  mas/yr down to  $R_F \simeq 18$ ) has been estimated from the formal errors of the fitted proper motions, while the zero point accuracy of the absolute proper motions have been tested by checking the mean motion of a set of known QSO's that give values smaller than 1 mas/yr on each component.

Radial velocities and chemical abundances of the sample of RR Lyræ and BHB giants were derived by means of spectroscopic observations carried out with the 4m Mayall telescope at Kitt Peak and with the 3.5m TNG on La Palma. The data were processed with standard procedures and routines (IRAF), and typical errors are  $\sigma_{RV} \leq 40$  km s $^{-1}$  and  $\sigma_{[Fe/H]} \sim 0.2$  dex.

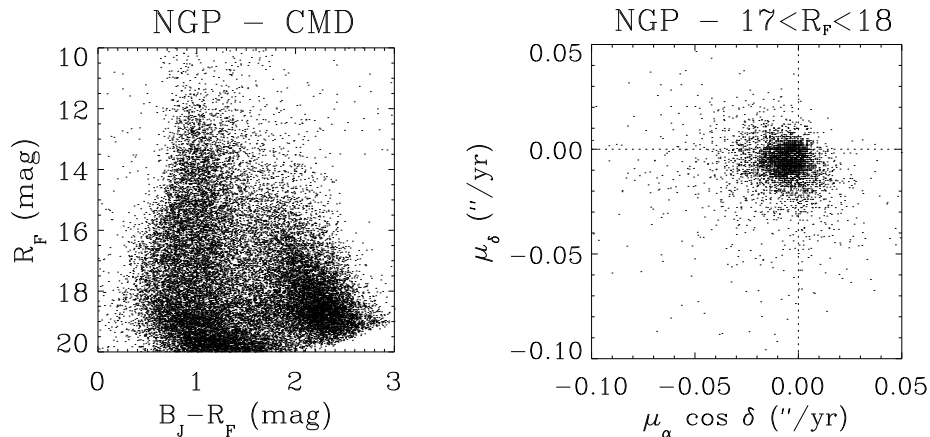


Figure 2. Color magnitude diagram (*left panel*) and vector point diagram (*right panel*) for stars with  $17 \leq R_F \leq 18$ . Both plots are based on data from the POSS-II field no. 442.

### 3. The vertical structure

The color magnitude diagram and the vector point diagram observed in one field of our NGP survey are shown in Figure 2. The observed distributions are the result of the complex mixture of the stars belonging to the various populations which are present towards high galactic latitudes. In particular, these may include:

1. the flat and rapidly rotating old thin disk,
2. the extended thick disk, including its metal weak tail,
3. a flattened and slowly rotating inner halo,
4. a spheroidal non-rotating outer halo,
5. satellite debris and kinematics substructures.

Actually, the physical properties of these components are not completely established and various problems are still controversial. For instance: (*a*) the density scale factor, rotation and metallicity distribution of the thick disk; (*b*) the nature of the metal weak thick disk (MWTD) and its relation with the standard thick disk (satellite debris or initial phase of a dissipative formation?); (*c*) the halo velocity ellipsoid, the spatial distribution and axial ratio of the halo as a function of the distance, (*d*) the search of halo streams; (*f*) the determination of the luminosity and mass function of the faintest Pop.II stars (white dwarfs, late M dwarfs and subdwarfs).

Due to the lack of trigonometric parallaxes for our and similar surveys, accurate distances and tangential velocities cannot be directly determined. In such a case it is convenient to analyze these large data-sets by comparing the observations against *ad hoc* Galaxy models which describe both the density and

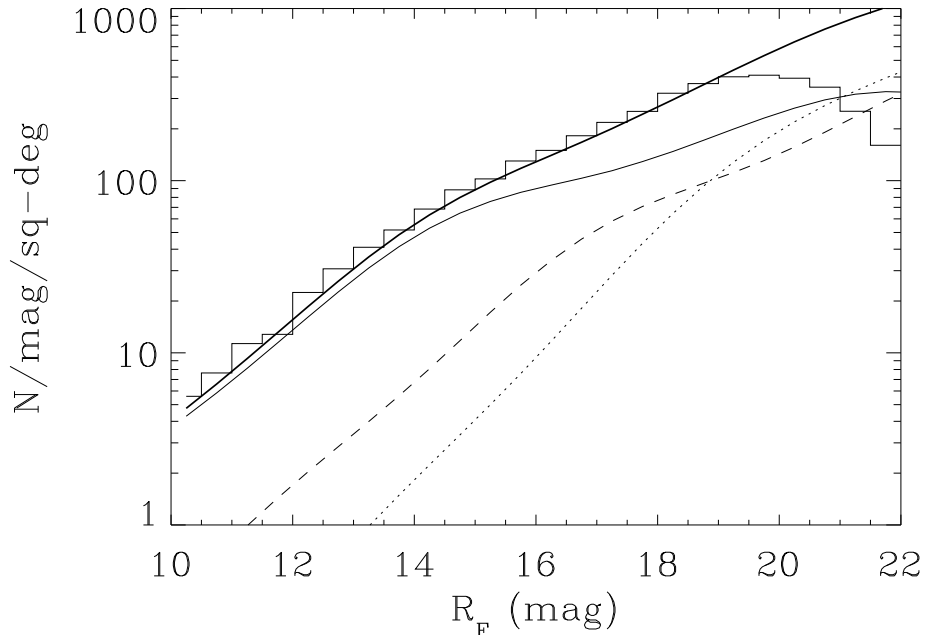


Figure 3. Starcounts derived from plate XP444 (*histogram*) and compared with the distribution predicted by the Galaxy model (*thick solid line*), which includes thin disk (*solid line*), thick disk (*dashed line*) and halo (*dotted line*) components.

kinematics, as for instance the Besançon model (Robin & Oblak 1987), the IAS Galaxy model (Bachall, Casertano & Ratnatunga 1987), or the models developed by Mendez & van Altena (1996) and Chen (1997). To this regard, in Figure 3 starcounts are compared against the Mendez’s Galaxy model which has been extended to the photographic  $B_J$  and  $R_F$  magnitudes by Spagna (2001).

Alternatively, using tracers with known brightness, it is possible to derive distance and space velocity by means of photometry, proper motions and spectroscopic radial velocities. This approach has been adopted to investigate the kinematics of the outer halo traced by a set of 31 RR Lyræ and 65 BHB giants, as will be discussed in the following section. These objects are distributed between  $2 \lesssim Z \lesssim 12$  kpc ( $V=12-16.5$  mag) and accurate photometric parallaxes ( $\sigma_d/d \lesssim 10\%$ ) have been computed by means of the  $M_V$  vs.  $B-V$  relation for BHB giants derived by Preston et al. (1991), while for RR Lyræ stars we adopted the  $M_V$  as a function of metallicity or of Fourier components, as follows:

$$M_V = 0.23 [\text{Fe}/\text{H}] + 0.92 \quad (1)$$

$$M_V = -1.876 \log P - 1.158A_1 + 0.821A_3 + 0.448 \quad (2)$$

where Eq. 1 is from Cacciari (2002) and Chaboyer (1999), while Eq. 2 is based on the relation from Kovács & Walker (2001) where  $P$  is the period (in days),

$A_1$  and  $A_3$  are the Fourier amplitudes (mag) of the fundamental and second harmonic components, respectively. The zero point has been calibrated by Kinman (2002) with respect to the absolute magnitude ( $M_V = 0.61_{-0.11}^{+0.10}$ ) of RR Lyr derived from the HST/FGS parallax measured by Benedict et al. (2002). Finally, the extinction  $E(B-V)$  has been estimated from the maps of Schlegel et al. (1998).

#### 4. Halo rotation

A retrograde rotation of the outer halo has been suggested by Majewski (1992) who measured a mean velocity  $\langle V \rangle = -275 \text{ km s}^{-1}$ , which corresponds to a galactocentric retrograde velocity  $v_{\text{rot}} \simeq -55 \text{ km s}^{-1}$  adopting  $V_{\text{LSR}} = 220 \text{ km s}^{-1}$ , from the analysis of a pure sample of halo subdwarfs at  $Z > 5.5 \text{ kpc}$  towards the NGP. As shown in Table 2, this parameter is still controversial, in fact Carney (1999), after correcting the kinematics bias of his kinematically-selected subdwarf sample, found a net prograde rotation of about  $\langle V \rangle = -196 \text{ km s}^{-1}$ . On the contrary, Chiba & Beers (2000) measured a prograde rotating inner halo,  $v_{\text{rot}} \simeq 20\text{-}60 \text{ km s}^{-1}$ , up to about 1 kpc, with a decreasing vertical gradient of  $dV/d|Z| = -52 \pm 6 \text{ km s}^{-1} \text{ kpc}^{-1}$ , while they did not detect any significant rotation above  $Z \sim 1.2 \text{ kpc}$  for very low abundance stars ( $-2.4 \leq [\text{Fe}/\text{H}] \leq -1.9$ ), where contamination of thick disk stars should be negligible. In addition, their halo sample at larger distances (212 stars with  $4 < Z_{\text{Max}} < 20 \text{ kpc}$  and  $[\text{Fe}/\text{H}] \leq -1.5$ ) still does not support any significant rotation:  $v_{\text{rot}} \simeq 0 \pm 8 \text{ km s}^{-1}$ .

Table 2. Recent measurements of the halo rotation.

Tracers	N.ro Objects	$\langle V \rangle$ (km/s)	Reference
INNER HALO			
RR Lyræ	162 ( $ Z  < 2 \text{ kpc}$ )	$-210 \pm 12^*$	Layden et al. (1996)
RR Lyræ	84 ( $ Z  < 2 \text{ kpc}$ )	$-219 \pm 10^*$	Martin & Morrison (1998)
RR Lyræ	147 ( $ Z  < 2 \text{ kpc}$ )	$-217 \pm 13^*$	Gould & Popowski (1998)
Subdwarfs	( $ Z  < 1 \text{ kpc}$ )	$-(160 \div 200)^{**}$	Chiba & Beers (2000)
OUTER HALO			
Subdwarfs	21 ( $Z > 4 \text{ kpc}$ )	$-275 \pm 16$	Majewski (1992)
Subdwarfs	30 ( $Z_{\text{Max}} > 5 \text{ kpc}$ )	$-196 \pm 13$	Carney (1999)
Subdwarfs	212 ( $Z_{\text{Max}} > 4 \text{ kpc}$ )	$-220 \pm 8$	Chiba & Beers (2000)
RR & BHB	53 ( $2 < Z < 12 \text{ kpc}$ )	$-285 \pm 17^{*,***}$	This survey

(\*) Heliocentric velocities. (Wrt. the LSR in the other cases.)

(\*\*) As a function of distance with a gradient  $dV/d|Z| = -52 \pm 6 \text{ km s}^{-1} \text{ kpc}^{-1}$  ( $-2.4 < [\text{Fe}/\text{H}] < -1.9$ ).

(\*\*\*) Preliminary results based on 18 RR Lyræ stars and 35 BHB giants).

However, recently Gilmore et al. (2002), who carried out a spectroscopic survey at intermediate galactic latitudes of about 2000 F/G stars, revealed a significant excess of *retrograde* halo stars in their faintest magnitude bin ( $18 < V < 19.5$ ) corresponding to a vertical distance  $|Z| \approx 5$  kpc.

The fact that the velocities of halo stars do not match an exact gaussian distribution is well known (see eg. Martin & Morrison 1998). How much this depends on the properties of the whole population or on the effects of kinematic substructures, such as satellite debris of ancient accretion events (eg. Helmi et al. 1999), remains to be established.

As shown in Table 2, a preliminary analysis of our sample of RR Lyræ and BHB giants (Kinman et al. 2002) seems to support a retrograde rotation of the outer halo. In fact, we measured a heliocentric velocity  $\langle V \rangle = -285 \pm 17$  km s<sup>-1</sup>, which corresponds to  $v_{\text{rot}} \simeq -60$  km s<sup>-1</sup> adopting a solar motion with respect to the LSR,  $V_{\odot} = +5.25 \pm 0.62$  km s<sup>-1</sup>, from Dehnen & Binney (1998) and assuming  $V_{\text{LSR}} = 220$  km s<sup>-1</sup>. This result is confirmed also by the separate analysis of the RR Lyræ and BHB giants, which both provide a retrograde rotation.

How much this value may be affected by a velocity bias can be estimated by the level of systematic errors on proper motions which in practice give the main contribution to the  $U$  and  $V$  galactic components along this line of sight towards  $b \approx 90^\circ$ . As reported in Sect. 2, we found systematic errors  $\Delta\mu < 1$  mas/yr, from which velocity bias up to 20-30 km s<sup>-1</sup> can be expected for such stars located at  $Z \approx 5$ -6 kpc, on average. Clearly, this is a critical point which need further analysis.

## 5. Kinematics simulation

A Montecarlo simulation has been developed in order to compare the GAIA capability to recover the halo kinematics with respect to the velocity precision that can be attained by the current and future ground based surveys. For simplicity we considered an uniform spatial distribution with Pop.II-like kinematics,  $(\sigma_U, \sigma_V, \sigma_W) = (150, 100, 100)$  km s<sup>-1</sup> and an observer rotating with a velocity of 220 km s<sup>-1</sup> at a distance of 8 kpc from the galactic center. Implicitly we assumed to measure bright tracers, such as RR Lyræ, BHB and red giants, having apparent magnitude  $V \sim 16$  mag at a distance of about  $d \sim 10$  kpc. The following cases were tested:

- Case A (GAIA), with  $\sigma_\pi = 10$   $\mu$ as,  $\sigma_\mu = 10$   $\mu$ as yr<sup>-1</sup> (per component) and  $\sigma_{V_r} = 10$  km s<sup>-1</sup>, from astrometric and spectroscopic observations;
- Case B (ground-based surveys), with  $\sigma_{m-M} = 0.2$  mag,  $\sigma_\mu = 1$  mas yr<sup>-1</sup> (per component) and  $\sigma_{V_r} = 10$  km s<sup>-1</sup>, from astrometric, photometric and spectroscopic observations.

Note that the two cases differ essentially in a factor 100 on the proper motion accuracy. In fact, at  $\sim 10$  kpc the distance accuracy is the same for both cases. This points out the fact that, although radial velocities and distance moduli derived from ground based spectro-photometric surveys can attain similar accuracy, GAIA astrometry will uniquely provide accurate and reliable tangential velocities up to large distances.

Figure 4 shows the results of Montecarlo simulations with 5000 stars towards  $b = 90^\circ$ . Top panels present the velocity errors (i.e. the differences between the observed velocity and the true value) for Case A, and those at the bottom for Case B. As expected, errors increase linearly with distance, and for GAIA the rms of  $\Delta U$  and  $\Delta V$  residuals vary from  $\sim 10 \text{ km s}^{-1}$  at 5 kpc to 20-30  $\text{km s}^{-1}$  at 10 kpc. For Case B the errors on U and V are about a factor 2-3 larger, while  $\sigma_{\Delta W} = \sigma_{V_r} \equiv 10 \text{ km s}^{-1}$  in both the cases. Note that in Case A the error on the tangential velocity is in practice dominated by the distance uncertainty,  $\sigma_\pi$ , while both the errors on proper motions and photometric parallaxes contribute to the velocity errors of Case B. Similar results are derived in other directions.

These velocity errors should be compared with the typical motion of the halo stars (100-200  $\text{km s}^{-1}$ ) for which GAIA will provide individual 3D spatial velocities with a significant signal-to-noise,  $\sigma_v/v$ , up to  $d \approx 10$ -15 kpc, a distance where ground based surveys are not able to measure reliable tangential velocities. GAIA will measure direct distances and velocities for large samples of halo tracers, selected *in situ* without kinematics nor metallicity bias, from which it will be possible to determine accurately the halo velocity ellipsoid and its orientation. In particular, the GAIA  $\mu$ -arcsec level accuracy will be essential in order to take advantage of the  $\sqrt{N}$  statistical factor and avoid the risk of velocity biases due to the presence of systematic errors affecting proper motions and parallaxes as discussed in Sect. 4.

Finally, accuracy of the order of 15-20  $\text{km s}^{-1}$ , such as that attained by GAIA for  $d \lesssim 10$  kpc, is the value requested to resolve kinematics substructures in the halo, as the satellite debris predicted by the hierarchical scenarios of galaxy formation. To this regards, Helmi (2002) estimated that GAIA will be able to recover 2/3 of the accretion events with a velocity accuracy better than 20  $\text{km s}^{-1}$  and  $\sigma_d/d < 20\%$  down to  $V \simeq 18.5$ , or 1/2 of the events down to  $V \simeq 15$  mag.

## 6. Summary

Large field proper motion surveys ( $\sigma_\mu \approx 1$ -10 mas/yr) based on photographic surveys digitized with fast measuring machines (APS, MAMA, PDS, PMM, SuperCOSMOS) are still useful tools for the study of the structure and kinematics of the galactic stellar populations, especially when combined with radial velocities and chemical abundances from spectro-photometric observations. In particular, we have shown how bright halo tracers, such as BHB giants and RR Lyræ stars with  $V \lesssim 16$ -17, can be used to investigate *in situ* the halo kinematics up to  $z \approx 5$ -6 kpc via photometric parallaxes if proper motions with  $\sigma_\mu \sim 1$ -2 mas/yr accuracy and radial velocities with precision of about  $\sigma_{V_r} \sim 10$ -20  $\text{km s}^{-1}$  are available. For statistical analysis of large samples, systematic errors on the proper motions (and  $M_V$  too) are critical and can result in biased mean velocities and dispersions. These problems will be dramatically reduced by the astrometric parameters and spectroscopic  $V_r$  provided by GAIA, which will permit to determine (a) direct distances from parallaxes, (b) radial and tangential velocities with an accuracy of a few tens of  $\text{km s}^{-1}$  to  $d \sim 10$ -15 kpc for (c) unbiased and larger sets of tracers identified by means of its spectro-photometric and astrometric data.



**Acknowledgments.** The GSC II is a joint project of the Space Telescope Science Institute and the Osservatorio Astronomico di Torino. Space Telescope Science Institute is operated by AURA for NASA under contract NAS5-26555. Partial financial support to this research comes from the Italian CNAA and the Italian Ministry of Research (MIUR) through the COFIN-2001 program.

## References

- Bachall, J.N., Casertano, S. & Ratnatunga K.U. 1987, ApJ, 320, 515
- Benedict, G.F., McArthur, B.E., Fredrick, L.W. et al. 2002, AJ, 123, 473
- Bucciarelli, B., Garcia Yus, J., Casalegno, R., Postman, M., Lasker, B. M., Sturch, C., Lattanzi, M.G., McLean, B.J., et al. 2001, A&A, 368, 335
- Chaboyer, B., 1999, in Post-Hipparcos cosmic candles, ed. A.Heck and F.Caputo, Kluwer Academic Pub. Boston, p.111
- Chen, B. 1997, ApJ, 491, 181
- Chiba, M., Beers, T.C., 2000, ApJ, 119, 2843
- Gould, A. & Popowski, P., 1998, ApJ, 508, 844
- Gilmore, G., Wyse, R.F.G. & Norris, J.E. 2002, ApJ, 574, L39
- Helmi, A., White, S.M., de Zeeuw, P.T. & Zhao H. 1999, Nature, 402, 52
- Helmi, A. 2002, in Second RVS meeting, Asiago 7-9 Feb. 2002  
<http://wwwhip.obspm.fr/gaia/rvs/bibliography/RVS-CoCo-003.pdf>
- Høg, E., Fabricius, C., Makarov, V.V., Urban, S., et al. 2000, A&A, 355, 27
- Kinman, T.D., Cacciari, C., Bragaglia A., Buzzoni, A. & Spagna, A. 2002, in EAS Publications Series, JENAM 2002, in press
- Kinman, T.D. 2002, in preparation
- Kovács, G. & Walker, A.R. 2001, A&A, 374, 264
- Lasker, B.M., McLean, B.J., Jenkner, H., Lattanzi, M.G., Spagna, A. 1995, in ESA SP-379, Future Possibilities for Astrometry in Space, Cambridge (UK), Jun 19-21, 1995, Ed. Perryman M.A.C., van Leeuwen F. & Guyenne T.-D., p. 137-141
- Majewski, S.R. 1992, ApJS, 78, 87
- McLean, B.J., Greene, G.R., Lattanzi, M.G., Pirenne, B. 2000, in ASP Conf. Ser. vol. 216, ADASS IX, Kohala Coast (HI, USA), Oct 3-6, 1999, Manset N., Veillet C. & Crabtree D. eds., 145-148
- Mendez, R.A. & van Altena, W.F. 1996, AJ, 112, 655
- Preston, G.W., Sheckman, S.A, Beers, T.C. 1991, ApJ, 375, 121
- Robin, A. & Oblak, E., 1987, in Proc. Xth IAU European Astronomy meeting, Vol.4, 323, Ed. J. Palous
- Schlegel, D.J., Finkbeiner Douglas, P. & Davis, M., 1998, ApJ, 500, 525
- Spagna, A. Lattanzi, M.G., Lasker, B.M., McLean, B.J., Massone, G., Lanteri, L. 1996, A&A, 311, 758
- Spagna, A., 2001, Guide Star Requirements for NGST: deep NIR Starcounts and Guide Star Catalogs, STScI-NGST-R-0013B, [http://www.ngst.nasa.gov/public/unconfigured/doc\\_0422/rev\\_03/NGST\\_GS\\_report5.pdf](http://www.ngst.nasa.gov/public/unconfigured/doc_0422/rev_03/NGST_GS_report5.pdf)

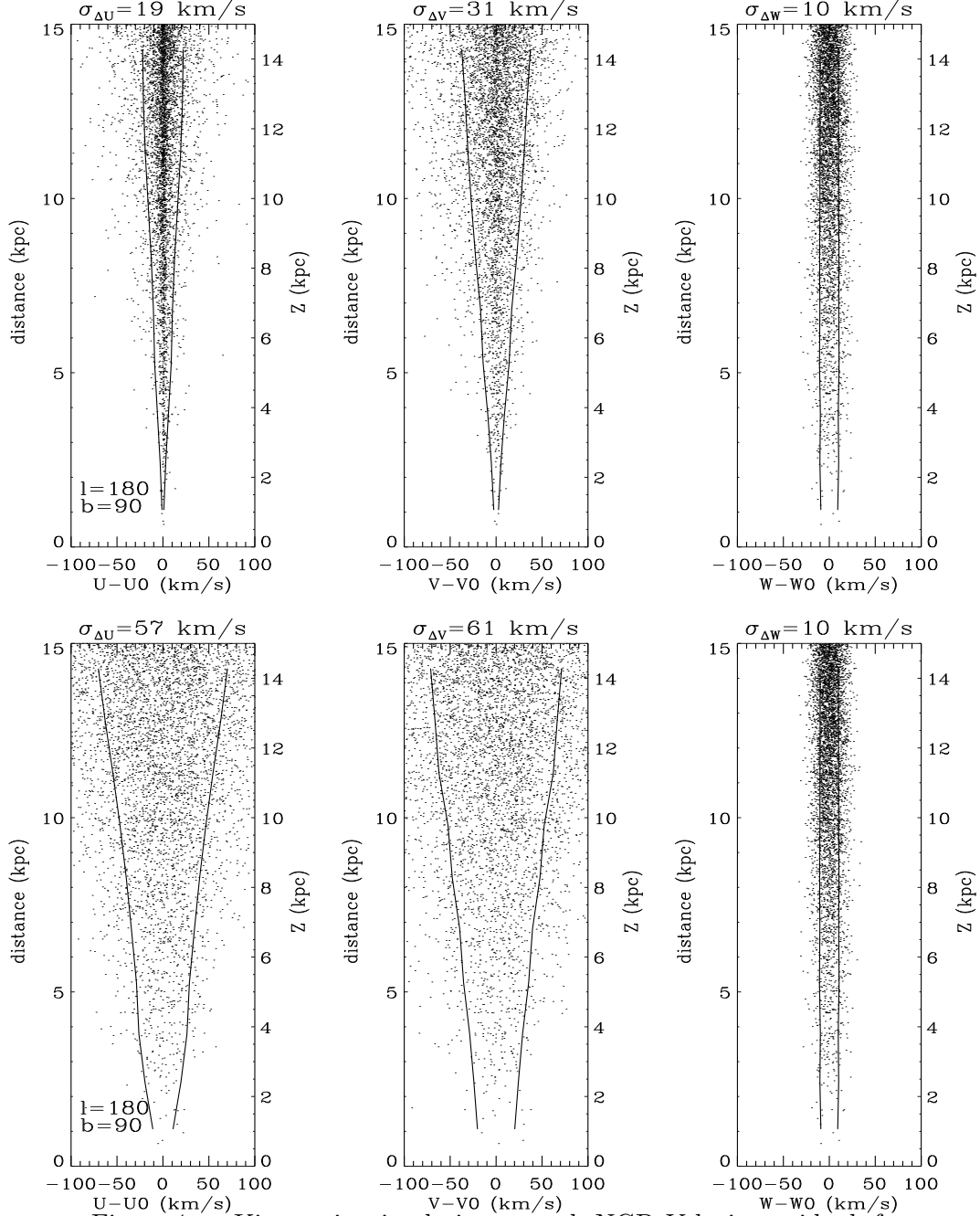


Figure 4. Kinematics simulation towards NGP. Velocity residuals for Case A (*top panels*) and Case B (*bottom panels*). Solid lines show the precision level ( $\pm 1\sigma$ ) as function of the distance up to  $Z=15$  kpc. Above each plot, the rms of the residuals of the whole sample is reported.